Original Article

Establishment of a Novel Mouse Model of Coronary Microembolization

Yuan-Yuan Cao[1], Zhang-Wei Chen[2], Jian-Guo Jia[2], Ao Chen[2], You Zhou[2], Yong Ye[2], Yan-Hua Gao[2], Yan Xia[2], Shu-Fu Chang[2], Jian-Ying Ma[2], Ju-Ying Qian[2], Jun-Bo Ge[2]

[1]Department of Cardiology, The Second Xiangya Hospital, Central South University, Changsha, Hunan 410011, China
[2]Department of Cardiology, Shanghai Institute of Cardiovascular Diseases, Zhongshan Hospital, Fudan University, Shanghai 200032, China

Yuan-Yuan Cao and Zhang-Wei Chen contributed equally to this work.

Abstract

Background: Coronary microembolization (CME) has been frequently seen in acute coronary syndromes and percutaneous coronary intervention. Small animal models are required for further studies of CME related to severe prognosis. This study aimed to explore a new mouse model of CME.

Methods: The mouse model of CME was established by injecting polystyrene microspheres into the left ventricular chamber during 15-s occlusion of the ascending aorta. Based on the average diameter and dosage used, 30 C57BL/6 male mice were randomly divided into five groups (n = 6 in each): 9 μm/500,000, 9 μm/800,000, 17 μm/200,000, 17 μm/500,000, and sham groups. The postoperative survival and performance of the mice were recorded. The mice were sacrificed 3 or 10 days after the surgery. The heart tissues were harvested for hematoxylin and eosin staining and Masson trichrome staining to compare the extent of inflammatory cellular infiltration and fibrin deposition among groups and for scanning transmission electron microscopic examinations to see the ultrastructural changes after CME.

Results: Survival analysis demonstrated that the cumulative survival rate of the 17 μm/500,000 group was significantly lower than that of the sham group (0/6 vs. 6/6, P = 0.001). The cumulative survival rate of the 17 μm/200,000 group was lower than those of the sham and 9 μm groups with no statistical difference (cumulative survival rate of the 17 μm/200,000, 9 μm/800,000, 9 μm/500,000, and sham groups was 4/6, 5/6, 6/6, and 6/6, respectively). The pathological alterations were similar between the 9 μm/500,000 and 9 μm/800,000 groups. The extent of inflammatory cellular infiltration and fibrin deposition was more severe in the 17 μm/200,000 group than in the 9 μm/500,000 and 9 μm/800,000 groups 3 and 10 days after the surgery. Scanning transmission electron microscopic examinations revealed platelet aggregation and adhesion, microthrombi formation, and changes in cardiomyocytes.

Conclusion: The injection of 500,000 polystyrene microspheres at an average diameter of 9 μm is proved to be appropriate for the mouse model of CME based on the general conditions, postoperative survival rates, and pathological changes.

Key words: Animal Model; Embolization; Mice; Microspheres

Introduction

In acute coronary syndromes, unstable atherothrombotic plaques contain more lipids and thrombi and less calcification. The microthrombi and debris cause the spontaneous embolization in coronary microcirculation. Iatrogenic rupture of atherosclerotic plaques during percutaneous coronary intervention can also result in coronary microembolization (CME), in spite of successful recanalization, leading to inadequate myocardial perfusion, continuous myocardial ischemia, progressive contractile dysfunction, and fatal arrhythmia.[1-4] The heavier the atherothrombotic burden, the greater the chances of CME. CME drew the attention of researchers about two decades ago with the awareness of its clinical frequency and importance.[5] Experimental animal models are required to understand

Access this article online

Quick Response Code:

Website: www.cmj.org

DOI: 10.4103/0366-6999.195469

Address for correspondence: Dr. Ju-Ying Qian, Department of Cardiology, Shanghai Institute of Cardiovascular Diseases, Zhongshan Hospital, Fudan University, Shanghai 200032, China
E-Mail: qian.juying@zs-hosptial.sh.cn

Received: 25-08-2016 **Edited by:** Yuan-Yuan Ji
How to cite this article: Cao YY, Chen ZW, Jia JG, Chen A, Zhou Y, Ye Y, Gao YH, Xia Y, Chang SF, Ma JY, Qian JY, Ge JB. Establishment of a Novel Mouse Model of Coronary Microembolization. Chin Med J 2016;129:2951-7.

the pathophysiological, morphological, molecular, and biological changes and to test the efficacy of new therapeutic interventions. Embolization by intracoronary infusion of microspheres into the coronary microcirculation has been used in large laboratory animals, mostly dogs and swine.[6-8] A mouse model of CME was established in the present study by an intraventricular injection of microspheres during occlusion of the ascending aorta.

Methods

Animal preparation and experimental protocol

Based on the average diameter and dosage used in CME, a total of 30 C57BL/6 male mice weighing 20–25 g were provided by the Department of Laboratory Animal Science, Fudan University, Shanghai, China, and kept under controlled conditions for temperature, humidity, and light, with standard chow and water available *ad libitum*. The mice were randomly divided into five groups: 9 μm/500,000, 9 μm/800,000, 17 μm/200,000, 17 μm/500,000, and sham groups. The study accorded with the *Guide for the Care and Use of Laboratory Animals* published by the US National Institutes of Health (NIH Publication No. 85-23, revised 1996), and it was approved by the Animal Care and Use Committee of Fudan University, China.

Preparation of polystyrene microspheres

The original liquid of white-stained polystyrene microspheres (Dynospheres; Dyno Particles, Lillestrøm, Norway) was diluted with the normal saline solution. Microspheres of both sizes were counted using a hemocytometer under an optical microscope to acquire different concentrations of microsphere diluents, including 500,000/50 μl and 800,000/50 μl for microspheres at an average diameter of 9 μm and 200,000/50 μl and 500,000/50 μl for microspheres at an average diameter of 17 μm. The preparations were shaken well before use.

Establishment of coronary microembolization model in mice

The mice were fully anesthetized with 2% inhalation isoflurane (Baxter International Inc., IL, USA) in oxygen, intubated and ventilated with a small animal ventilator (Type 7025, Ugo Basile, Comerio, Italy) at 100 breaths per minute. Anesthesia of the mice was maintained with the inhalation of 1.5% isoflurane during the procedures. The heart and the ascending aorta were exposed through a middle line thoracotomy and then a sternotomy at the second and third intercostal spaces. A silk suture (size #5) was placed afterward under the aortic root for occluding the ascending aorta [Figure 1a]. Subsequently, diluted white-stained polystyrene microspheres at a volume of 50 μl with different diameters and dosages were injected as a bolus with a 29-gauge needle into the left ventricular chamber during 15-s occlusion of the ascending aorta [Figure 1b]. Then, the thoracic cavity and the skin incision were closed successively with sutures. An identical procedure was performed in the sham group with saline injected instead of microspheres.

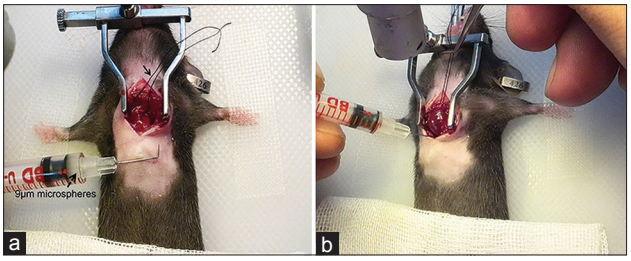

Figure 1: Procedures of mouse coronary microembolization modeling. (a) A #5 silk suture has been placed under the aortic root (solid arrow) after thoracotomy, and 500,000 white-stained polystyrene microspheres with an average diameter of 9 μm at a volume of 50 μl have been prepared (dotted arrow). (b) The injection of microspheres into the left ventricular chamber from the apex while the ascending aorta was occluded.

General observations after operation

All the mice after operation were kept under standard controlled conditions. The general conditions and mobility, as well as the number of the surviving and dead mice, were observed and recorded every day.

Histological analyses and electron microscopic detections

The surviving mice were sacrificed by cervical dislocation 3 and 10 days after the surgery. The heart tissues were harvested for histological examinations and scanning transmission electron microscopic detections. For all the cases of unexpected death, thoracotomy was performed to see whether operation-related complications such as massive bleeding or pulmonary artery or aorta injury existed. The heart tissues of the mice were acquired and sent for histological analyses as soon as possible. Most heart tissues were fixed with 10% formaldehyde, embedded in paraffin, and then sectioned into slices of 5 μm thickness for hematoxylin and eosin (HE) staining and Masson trichrome staining. The slices were examined by light microscopy. An average of three slices from different parts of the heart of every mouse were analyzed for the extent of inflammatory cellular infiltration and fibrin deposition using the ImagePro Plus 6.0 software (Media Cybernetics, Inc., MD, USA). The extent of inflammatory cellular infiltration was expressed as a percentage calculated by dividing the area of inflammatory cellular infiltration by the total area of heart tissue in the slice; the same algorithm was used for the degree of fibrin deposition. A small part of heart tissues from every mouse was processed and fixed with 2.5% glutaraldehyde and then delivered to the Electron Microscope Room, Shanghai Medical College, Fudan University, for scanning transmission electron microscope detections to observe ultrastructural changes. The brain tissues of the paralyzed mice after operation were also collected for HE staining. Moreover, the kidney tissues of the mice from CME groups were harvested for HE staining to understand the distribution of the microspheres in the systemic circulation.

Statistical analysis

Statistical analyses were performed using Stata software (version 10.0, Stata Corp., TX, USA). Gaussian distribution

data were presented as mean ± standard deviation. Categorical variables were expressed as frequencies and percentages. Survival analysis was done by Kaplan–Meier method. Groups were compared by one-way analysis of variance, and Bonferroni's test was performed to identify differences between groups. All *P* values were two-sided, and $P < 0.05$ was considered statistically significant.

Results

General conditions and survival analyses

All the mice in the sham and 9 μm/500,000 groups survived. One mouse (1/6) in the 9 μm/800,000 group and one (1/6) in the 17 μm/500,000 group had poor performance after CME. They barely ate, drank, or moved even when stimulated. The two mice died several hours after the operation. No massive bleeding in the chest or pulmonary artery or aorta injuries was observed. The others (5/6) in the 9 μm/800,000 group survived. Two mice (2/6) in the 17 μm/500,000 group and one (1/6) in the 17 μm/200,000 group were paralyzed, presenting with the abnormality in the right hind leg movement and inability to feed themselves; they died the next day. Moreover, three mice (3/6) in the 17 μm/500,000 group and one (1/6) in the 17 μm/200,000 group died immediately due to cardiac arrest after injecting the microspheres. The others (4/6) in the 17 μm/200,000 group survived. In consequence of the unexpected deaths, three, two, one, and three mice were finally sacrificed 3 days after the surgery in the 9 μm/500,000, 9 μm/800,000, 17 μm/200,000, and sham groups, respectively; three mice in each of these groups were sacrificed 10 days after the surgery. Survival analysis demonstrated that the cumulative survival rate of the 17 μm/500,000 group was significantly lower than that of the sham group (0/6 vs. 6/6, $P = 0.001$) [Figure 2]. The cumulative survival rate of the 17 μm/200,000 group was lower than those of the sham and 9 μm groups (cumulative survival rate of the 17 μm/200,000, 9 μm/800,000, 9 μm/500,000, and sham groups was 4/6, 5/6, 6/6, and 6/6, respectively), but the statistical difference was not significant (17 μm/200,000 vs. sham, $P = 0.139$).

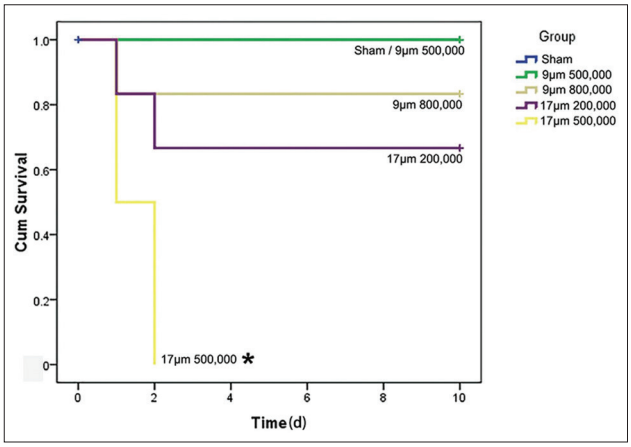

Figure 2: Survival analysis of coronary embolization with different sizes and quantities ($n = 6$ in each group). *Compared to the sham group, the cumulative survival rate was significantly lower in the 17 μm/500,000 group ($P = 0.001$). There were no significant differences among the 17 μm/200,000, 9 μm/800,000, 9 μm/500,000, and sham groups.

Histopathological findings

HE staining showed numerous microspheres in the coronary microcirculation without obvious inflammatory cell infiltration in the 17 μm/500,000 group on both the day and the next day of CME. Masson trichrome staining also showed no significant collagen deposition [Figure 3]. Multiple myocardial necroses of varying sizes with inflammatory cell infiltration and collagen deposition were revealed in all the CME groups 3 and 10 days after the surgery. These changes were not observed in the sham group [Figures 4-7]. Histopathological examinations showed significant inflammatory infiltration and collagen deposition 3 and 10 days after the surgery in the 17 μm/200,000 (inflammatory infiltration: 15.16% ± 7.73% at day 10; collagen deposition: 16.27% ± 5.74% at day 10), 9 μm/800,000 (inflammatory infiltration: 9.11% ± 4.96% at day 10; collagen deposition: 9.19% ± 4.52% at day 10), and 9 μm/500,000 groups (inflammatory infiltration: 10.43% ± 5.86% at day 10; collagen deposition: 9.15% ± 4.81% at day 10) compared with the sham group (inflammatory infiltration: 1.24% ± 0.23% at day 10; collagen deposition: 1.21% ± 0.17% at day 10). The extent of inflammatory cellular infiltration and collagen deposition in the 17 μm/200,000 group was more severe than that in the 9 μm/800,000 and 9 μm/500,000 groups, both 3 and 10 days after the surgery. No significant differences in histopathological variations were observed between the 9 μm/800,000 and 9 μm/500,000 groups [Figures 8 and 9].

A few singular microspheres were found in the kidney specimens of both the 9 μm and 17 μm groups [Figure 10]. HE staining of the brain tissues of the paralyzed mice revealed numerous microspheres at an average diameter of 17 μm accompanied by a disorganized structure of brain tissues and focal vacuole-like changes [Figure 11].

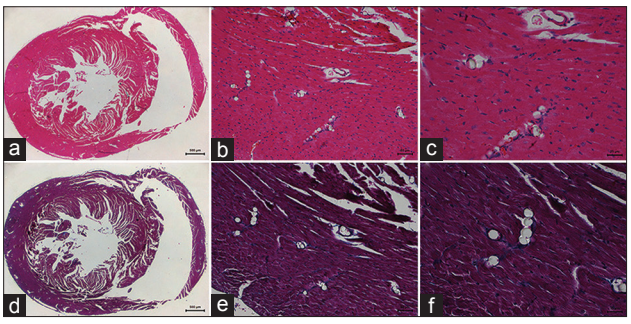

Figure 3: The representative images of myocardium of the left ventricle with HE staining or Masson trichrome staining in 17 μm/500,000 group 1 day after coronary microembolization operation. (a-c) Images in HE staining, with original magnification ×25, ×200, and ×400, respectively; (d-f) Images in Masson trichrome staining, with original magnification ×25, ×200, and ×400, respectively. Numerous microspheres filled in the coronary microcirculation without obvious inflammatory cell infiltration or collagen deposition.

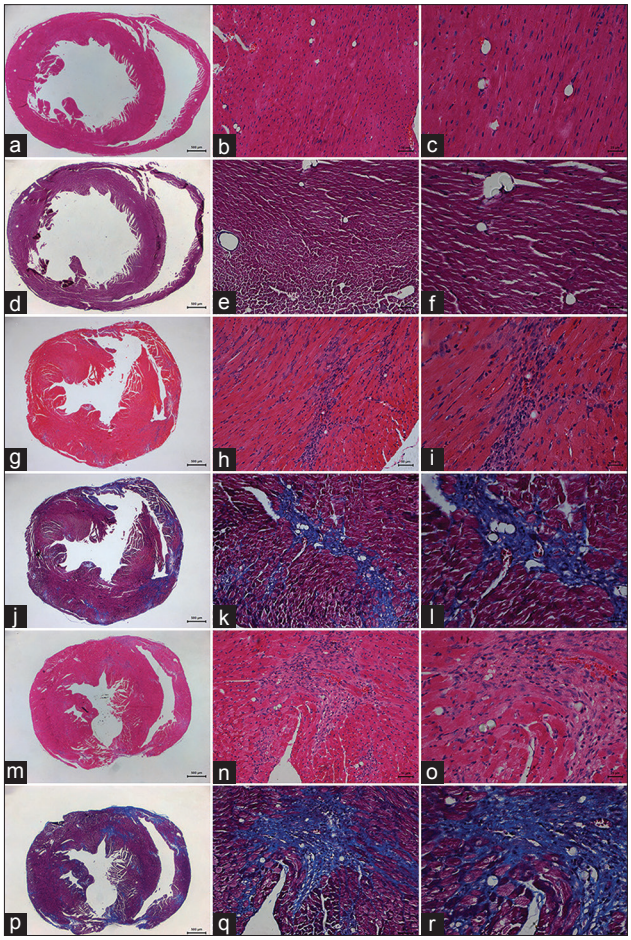

Figure 4: The representative images of myocardium of the left ventricle with HE staining or Masson trichrome staining in 17 μm/200,000 group 1, 3, and 10 days after the surgery. (a-c) Images in HE staining 1 day after the surgery, with original magnification ×25, ×200, and ×400, respectively; (d-f) Images in Masson trichrome staining 1 day after surgery, with original magnification ×25, ×200, and ×400, respectively. (g-l) 3 days after the surgery and (m-r) 10 days after the surgery. The images showed myocardial necroses of varying sizes with inflammatory cell infiltration and collagen deposition 3 and 10 days after the surgery in 17 μm/200,000 group.

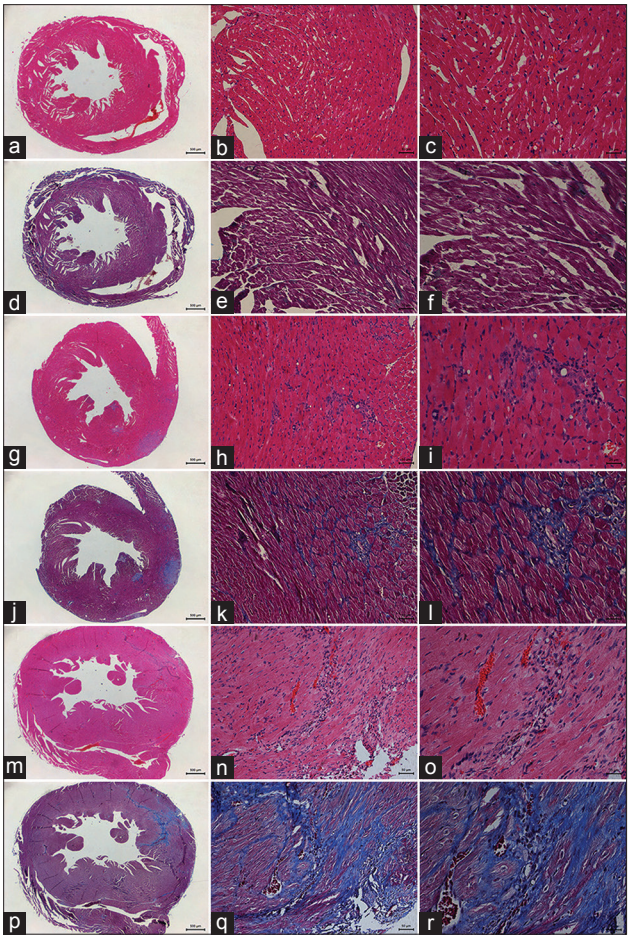

Figure 5: The representative images of myocardium of the left ventricle with HE staining or Masson trichrome staining in the 9 μm/800,000 group 1, 3, and 10 days after the surgery. (a-c) Images in HE staining 1 day after the surgery, with original magnification ×25, ×200, and ×400, respectively; (d-f) Images in Masson trichrome staining 1 day after the surgery, with original magnification ×25, ×200, and ×400, respectively; (g-l) 3 days after the surgery and (m-r) 10 days after the surgery. The images showed myocardial necroses of varying sizes with inflammatory cell infiltration and collagen deposition 3 and 10 days after the surgery in the 9 μm/800,000 group.

Scanning transmission electron microscopic detections

The neatly arranged myoneme and densely distributed mitochondria were observed in the normal myocardium [Figure 12a and 12b]. Polystyrene microspheres were packed in capillaries [Figure 12c], accompanied by platelet adhesion [Figure 12g], aggregation [Figure 12h], and microthrombi formation [Figure 12g and 12h] in the coronary embolization group. The integrity of focal myocardial cells was destroyed [Figure 12e and 12f]. Mitochondrial swelling [Figure 12d], release of organelles, disorganized myocardial fibers, widened intercellular space [Figure 12e and 12f], and inflammatory cell infiltration [Figure 12h] were detected. These observations were more frequently found 3 days after the surgery.

Discussion

To the best of our knowledge, mice have seldom been used to construct the model of CME so far. This study attempted and succeeded to produce a mouse model of CME. The present study demonstrated that the mouse model of CME could be established by the unselective intracoronary fusion of polystyrene microspheres with the occluded ascending aorta through injection from the apex. Different sizes and dosages of the microspheres were compared to determine the optimum one. The operation could be successfully done with a high survival rate in the 9 μm/500,000 group. Based on the general conditions, postoperative survival rates, and histopathological changes, 500,000 polystyrene microspheres at an average diameter of 9 μm proved to be the most appropriate to establish the mouse model of CME.

Lycopodium spores were the first materials to be used to embolize coronary arteries to induce myocardial ischemia.[9] Then, different sizes of microspheres replaced

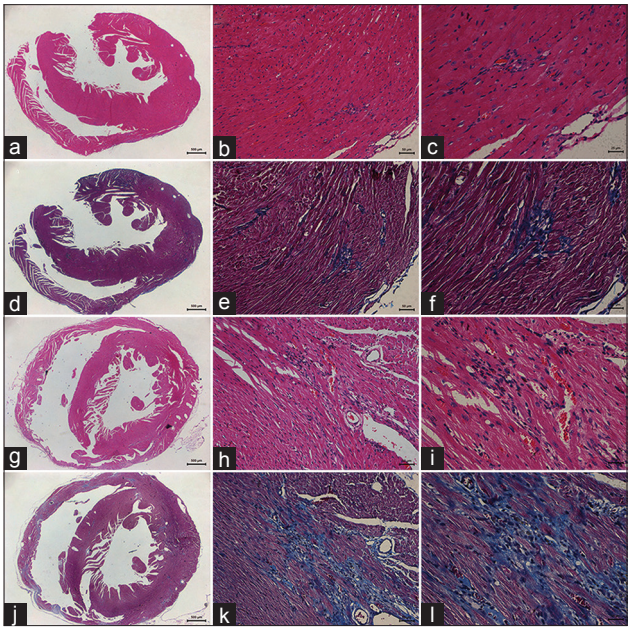

Figure 6: The representative images of myocardium of the left ventricle with HE staining or Masson trichrome staining in the 9 μm/500,000 group 3 and 10 days after the surgery. (a-c) Images in HE staining 3 days after the surgery, with original magnification ×5, ×200, and ×400, respectively; (d-f) Images in Masson trichrome staining 3 days after the surgery, with original magnification ×25, ×200, and ×400, respectively; (g-l) 10 days after the surgery. The images showed myocardial necroses of varying sizes with inflammatory cell infiltration and collagen deposition 3 and 10 days after the surgery in the 9 μm/500,000 group.

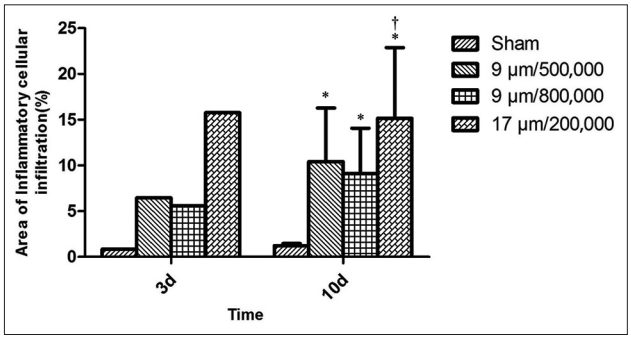

Figure 8: Comparison of inflammatory cellular infiltration area among groups. Compared to the sham group, the other three groups had significant inflammatory infiltration 3 and 10 days after the surgery (*$P < 0.05$); there was no significant difference between the 9 μm/800,000 and 9 μm/500,000 groups; the area of inflammatory cellular infiltration was more in the 17 μm/200,000 group than 9 μm/800,000 and 9 μm 500,000 groups 3 and 10 days after the surgery (†$P < 0.05$).

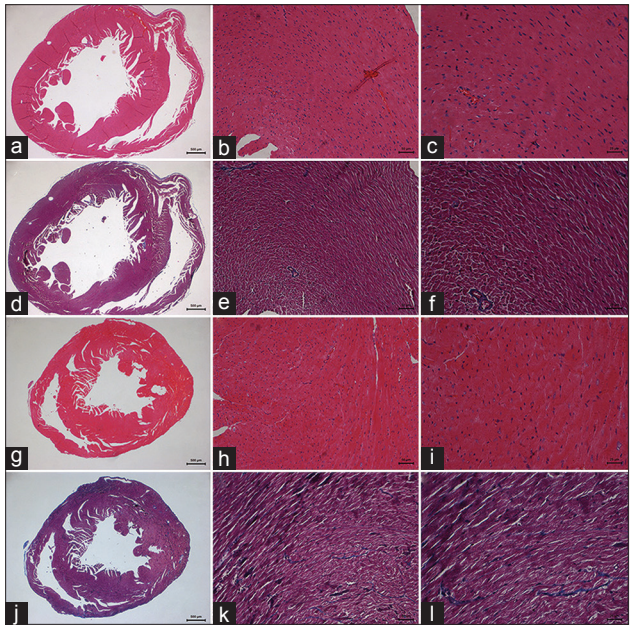

Figure 7: The representative images of myocardium of the left ventricle with HE staining or Masson trichrome staining in the sham group 3 and 10 days after the surgery. (a-c) Images in HE staining 3 days after the surgery, with original magnification ×25, ×200, and ×400, respectively; (d-f) Images in Masson trichrome staining 3 days after the surgery, with original magnification ×25, ×200, and ×400, respectively; (g-l) 10 days after the surgery. The images showed no obvious microinfarct formation.

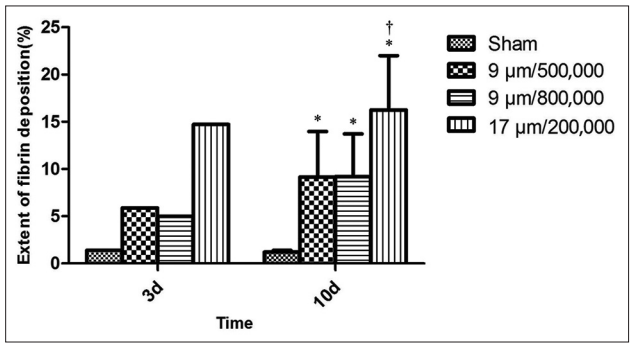

Figure 9: Comparison of the extent of fibrin deposition among groups. Compared to the sham group, the other three groups had significant fibrin deposition 3 and 10 days after the surgery (*$P < 0.05$); there was no significant difference between the 9 μm/800,000 and 9 μm/500,000 groups; the extent of fibrin deposition was more severe in the 17 μm/200,000 group than 9 μm/800,000 and 9 μm 500,000 groups 3 and 10 days after the surgery (†$P < 0.05$).

the lycopodium spores and were widely applied in the experimental coronary embolization.[10] Nevertheless, lycopodium spores or microspheres did not resemble microemboli found in the hearts of patients who died of sudden death or acute coronary syndrome at autopsy. Microemboli found in the coronary microcirculation of patients were associated with multifocal microinfarcts.[11,12] The microemboli, composed of platelets, fibrin, hemocytes, and atherosclerotic plaque materials, including cholesterol crystals, induced a marked inflammatory response characterized by leukocyte infiltration.[12] The components of the microemboli can trigger biological responses and interact with each other. However, microspheres are chemically inert and nonfunctional pathophysiologically and biologically. It is hard to duplicate the pathophysiological process of CME because the microemboli identified in the patients who suffered from sudden death or acute coronary syndrome cannot be reproduced. However, the use of microspheres in animals induces similar microinfarcts as reported in

the patients' hearts, which was confirmed in the present mouse model of CME. Platelet adhesion, aggregation, and microthrombi formation, accompanied by the myocardial cell injury, were detected by scanning transmission electron microscopy. Moreover, the area of the microinfarcts induced by 9 μm/500,000 microspheres in the present study was similar to that in the widely used pig models.[6,13]

Li *et al*.[14] have recently reported the application of homologous thrombotic material to produce rat CME models. The homologous microthrombotic particles were prepared based on the venous blood clotting, followed by screening out of the particles with appropriate sizes through a filter. However, the preparation of microthrombotic particles complicates the rat model establishment. Nevertheless, these microthrombotic particles lack *in situ* thrombosis and vascular endothelial injuries. Sodium laurate can cause vascular endothelial damage and *in situ* thrombosis. Therefore, it has been used in constructing rat models of coronary artery microthrombosis,[15] cerebral infarction,[16] and peripheral arterial occlusive disease.[17] Injection of sodium laurate can cause more severe myocardial infarct and inflammation compared with microspheres. Moreover, sodium laurate goes into systemic circulation and destroys the integrity of vascular walls, followed by serious and progressive *in situ* thrombosis and organ dysfunction. Hence, it seems that an ideal animal model of CME does not exist at present.

A marked difference exists between big and small animals in the method of injecting microspheres. For big animals, such as dogs, swine, mini swine, calves,[18] and sheep,[19] a selective injection of microspheres into the coronary artery, usually the left anterior descending artery, can be easily accomplished through coronary angiography,[13,20,21] which is not feasible in small animals because of smaller vessels. Therefore, the unselective way is more suitable for small animals.[22] However, it may cause potential and inevitable injuries to other organs, such as the brain and kidneys, because the remaining microspheres in the left ventricle go into the systemic circulation with blood flow after opening the aorta. Hence, it was supposed that 9 μm/500,000 microspheres were better because fewer microspheres would go into the systemic circulation although the degree of microinfarction in the 9 μm/800,000 and 9 μm/500,000 groups was similar.

The present study had a few limitations. First, the sample size was small that may have an undesirable influence on the results. Further studies were needed to verify the results. Electrocardiographic changes after operation were not monitored. CME might cause severe, fatal arrhythmia.

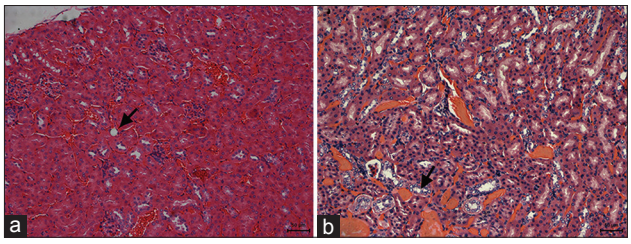

Figure 10: The representative images of kidney tissue with HE staining (original magnification ×200). (a) The 17 μm/200,000 group; (b) 9 μm/500,000 group. A few singular microspheres (arrow) were found in these kidney specimens, indicating part of the microspheres went into the systemic circulation with blood flow.

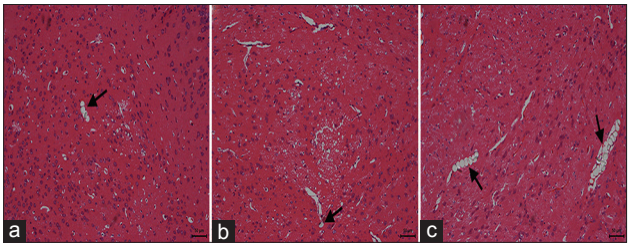

Figure 11: The representative images of brain tissue of the paralyzed mice in the 17 μm/200,000 group with HE staining (original magnification ×200). (a-c) Plentiful microspheres at an average diameter of 17 μm (arrow) accompanied by disorganized structure of brain tissues, and focal vacuole-like changes were observed.

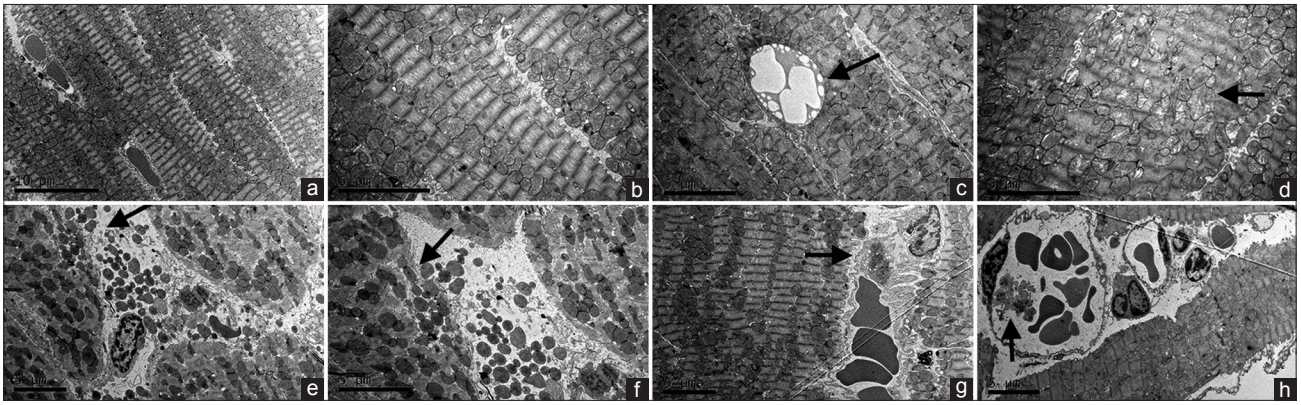

Figure 12: The representative images of ultrastructural changes observed under scanning transmission electron microscope. (a and b) Normal ultrastructure in the sham group; (c) the arrow indicates polystyrene microspheres packed in capillaries; (d) the arrow indicates swelling mitochondria; (e) the arrow indicates destroyed myocardiocyte and organelles release; (f) the arrow indicates the ruptured myocardial cell membrane; (g) the arrow indicates platelet adhesion and microemboli formation; (h) the arrow indicates platelet aggregation and leukocytes outside of the vessel. The scale bar in (a) indicates 10 μm; the scale bars in (b-h) indicate 5 μm.

Moreover, a full autopsy was not performed for every mouse, which might have provided more comprehensive information to understand the deaths and the degree of embolization of other organs in this study.

In conclusion, the present mouse model with appropriate microspheres might promote further studies on coronary embolization compared with complicated and time-consuming big animal models.

Financial support and sponsorship

This study was supported by grants from the National Natural Science Foundation of China (No. 81570314, 81200146, and 81370322), the Zhongshan Hospital Excellent Backbone (No. 2015ZSYXGG07), the Zhongshan Hospital Youth Science (No. 2012ZSQN12), the New Teacher Foundation of Ministry of Education (No. 20120071120061), the Shanghai Municipal Science and Technology Commission (No. 15XD1501100), and the Shanghai Municipal Commission of Health and Family Planning (No. XBR2013071 and 20134001).

Conflicts of interest

There are no conflicts of interest.

References

1. Fokkema ML, Vlaar PJ, Svilaas T, Vogelzang M, Amo D, Diercks GF, *et al.* Incidence and clinical consequences of distal embolization on the coronary angiogram after percutaneous coronary intervention for ST-elevation myocardial infarction. Eur Heart J 2009;30:908-15. doi: 10.1093/eurheartj/ehp033.
2. Henriques JP, Zijlstra F, Ottervanger JP, de Boer MJ, van't Hof AW, Hoorntje JC, *et al.* Incidence and clinical significance of distal embolization during primary angioplasty for acute myocardial infarction. Eur Heart J 2002;23:1112-7. doi: 10.1053/euhj.2001.3035.
3. Herrmann J. Peri-procedural myocardial injury: 2005 update. Eur Heart J 2005;26:2493-519. doi: 10.1093/eurheartj/ehi455.
4. Napodano M, Ramondo A, Tarantini G, Peluso D, Compagno S, Fraccaro C, *et al.* Predictors and time-related impact of distal embolization during primary angioplasty. Eur Heart J 2009;30:305-13. doi: 10.1093/eurheartj/ehn594.
5. Heusch G, Kleinbongard P, Böse D, Levkau B, Haude M, Schulz R, *et al.* Coronary microembolization: From bedside to bench and back to bedside. Circulation 2009;120:1822-36. doi: 10.1161/CIRCULATIONAHA.109.888784.
6. Chen ZW, Qian JY, Ma JY, Chang SF, Yun H, Jin H, *et al.* TNF-α-induced cardiomyocyte apoptosis contributes to cardiac dysfunction after coronary microembolization in mini-pigs. J Cell Mol Med 2014;18:1953-63. doi: 10.1111/jcmm.12342.
7. Eng C, Cho S, Factor SM, Sonnenblick EH, Kirk ES. Myocardial micronecrosis produced by microsphere embolization. Role of an alpha-adrenergic tonic influence on the coronary microcirculation. Circ Res 1984;54:74-82.
8. Monroe RG, LaFarge CG, Gamble WJ, Kumar AE, Manasek FJ. Left ventricular performance and coronary flow after coronary embolization with plastic microspheres. J Clin Invest 1971;50:1656-65. doi: 10.1172/JCI106655.
9. Hamburger WW, Priest WS, Bettman RB. Experimental coronary embolism. Am J Med Sci 1926;171:168-85.
10. Heusch G, Schulz R, Baumgart D, Haude M, Erbel R. Coronary microembolization. Prog Cardiovasc Dis 2001;44:217-30. doi: 10.1053/pcad.2001.26968.
11. El-Maraghi N, Genton E. The relevance of platelet and fibrin thromboembolism of the coronary microcirculation, with special reference to sudden cardiac death. Circulation 1980;62:936-44.
12. Falk E. Unstable angina with fatal outcome: Dynamic coronary thrombosis leading to infarction and/or sudden death. Autopsy evidence of recurrent mural thrombosis with peripheral embolization culminating in total vascular occlusion. Circulation 1985;71:699-708.
13. Carlsson M, Wilson M, Martin AJ, Saeed M. Myocardial microinfarction after coronary microembolization in swine: MR imaging characterization. Radiology 2009;250:703-13. doi: 10.1148/radiol.2503081000.
14. Li S, Zhong S, Zeng K, Luo Y, Zhang F, Sun X, *et al.* Blockade of NF-kappaB by pyrrolidine dithiocarbamate attenuates myocardial inflammatory response and ventricular dysfunction following coronary microembolization induced by homologous microthrombi in rats. Basic Res Cardiol 2010;105:139-50. doi: 10.1007/s00395-009-0067-6.
15. Fang KF, Chen ZJ, Liu M, Wu PS, Yu DZ. Blood pH in coronary artery microthrombosis of rats. Asian Pac J Trop Med 2015;8:864-9. doi: 10.1016/j.apjtm.2015.09.015.
16. Chen Y, Ge J W, Deng BX. A new rat model of cerebral infarction based on the injury of vascular endothelial cell (in Chinese). Chin J Integr Med 2005;11:195-200.
17. Ashida S, Ishihara M, Ogawa H, Abiko Y. Protective effect of ticlopidine on experimentally induced peripheral arterial occlusive disease in rats. Thromb Res 1980;18:55-67.
18. Weber KT, Malinin TI, Dennison BH, Fuqua JM Jr., Speaker DM, Hastings FW. Experimental myocardial ischemia and infarction. Production of diffuse myocardial lesions in unanesthetized calves. Am J Cardiol 1972;29:793-802.
19. Ikram H, Rogers SJ, Charles CJ, Sands J, Richards AM, Bridgman PG, *et al*. An ovine model of acute myocardial infarction and chronic left ventricular dysfunction. Angiology 1997;48:679-88.
20. Chen Z, Qian J, Ma J, Chang S, Yun H, Jin H, *et al.* Glucocorticoid ameliorates early cardiac dysfunction after coronary microembolization and suppresses TGF-ß1/Smad3 and CTGF expression. Int J Cardiol 2013;167:2278-84. doi: 10.1016/j.ijcard.2012.06.002.
21. Ma JY, Qian JY, Jin H, Chen ZW, Chang SF, Yang S, *et al*. Acute hyperenhancement on delayed contrast-enhanced magnetic resonance imaging is the characteristic sign after coronary microembolization. Chin Med J 2009;122:687-91.
22. Li L, Qu N, Li DH, Wen WM, Huang WQ. Coronary microembolization induced myocardial contractile dysfunction and tumor necrosis factor–α mRNA expression partly inhibited by SB203580 through a p38 mitogen-activated protein kinase pathway. Chin Med J 2011;124:100-5.